Inorg. Chem. **2004**, *43*, 4080–4090

Role of Solvation in the Reduction of the Uranyl Dication by Water: A Density Functional Study

Lyudmila V. Moskaleva, Sven Krüger, Andreas Spörl, and Notker Rösch*

Institut für Physikalische und Theoretische Chemie, Technische Universität München, 85747 Garching, Germany

Received December 17, 2003

We have studied the solvation of uranyl, UO_2^{2+}, and the reduced species $UO(OH)^{2+}$ and $U(OH)_2^{2+}$ systematically using three levels of approximation: direct application of a continuum model (M1); explicit quantum-chemical treatment of the first hydration sphere (M2); a combined quantum-chemical/continuum model approach (M3). We have optimized complexes with varying numbers of aquo ligands ($n = 4$–6) and compared their free energies of solvation. Models M1 and M2 have been found to recover the solvation energy only partially, underestimating it by ∼100 kcal/mol or more. With our best model M3, the calculated hydration free energy $\Delta_h G°$ of UO_2^{2+} is about –420 kcal/mol, which shifts to about –370 kcal/mol when corrected for the expected error of the model. This value agrees well with the experimentally determined interval, –437 kcal/mol < $\Delta_h G°$ < –318 kcal/mol. Complexes with 5 and 6 aquo ligands have been found to be about equally favored with models M2 and M3. The same solvation models have been applied to a two-step reduction of UO_2^{2+} by water, previously theoretically studied in the gas phase. Our results show that the solvation contribution to the reaction free energy, about 60 kcal/mol, dominates the endoergicity of the reduction.

Introduction

Investigations on the structure and properties of actinide compounds are becoming increasingly important due to the growing problem of nuclear waste accumulation and its penetration into the environment. Until the past decade, theoretical studies of these heavy elements were scarce because their high nuclear charge entails many challenges: relativistic effects including the spin−orbit interaction as well as the correlation energy of many electrons that have to be treated explicitly. An additional complication arises from the fact that most of the relevant chemistry of actinides takes place in solution, and therefore, bulk solvent effects need to be taken into account. Recently, however, progress in quantum chemical methods, especially those based on density functional theory (DFT), and improved computational facilities stimulated a renewed interest in this area. Now, computational studies are no longer limited to benchmark calculations on halides or oxo cations but can be extended to chemically more interesting, albeit more complex, coordination compounds of U, as well as Np and Pu, which are relevant to actinide speciation in the environment.[1−16]

Solvent effects, treated at various degrees of sophistication, were applied to study the coordination environment and

* Author to whom correspondence should be addressed. E-mail: roesch@theochem.tu-muenchen.de.

(1) Spencer, S.; Gagliardi, L.; Handy, N. C.; Ioannou, A. G.; Skylaris, C.-K.; Willets, A.; Simper, A. M. *J. Phys. Chem. A* **1999**, *103*, 1831−1837.
(2) Tsushima, S.; Suzuki, A. *THEOCHEM* **2000**, *529*, 21−25.
(3) Tsushima, S.; Yang, T.; Suzuki, A. *Chem. Phys. Lett.* **2001**, *334*, 365−373.
(4) Hay, P. J.; Martin, R. L.; Schreckenbach, G. J. *J. Phys. Chem. A* **2000**, *104*, 6259−6270.
(5) Wahlgren, U.; Moll, H.; Reich, T.; Geipel, G.; Grenthe, I.; Schimmelpfennig, B.; Maron, L.; Vallet, V.; Gropen, I. *J. Phys. Chem. A* **1999**, *103*, 8257−8264.
(6) Farkas, I.; Bányai, I.; Szabó, Z.; Wahlgren, U.; Grenthe I. *Inorg. Chem.* **2000**, *39*, 799−805.
(7) Vallet, V.; Wahlgren, U.; Schimmelpfennig, B.; Szabó, Z.; Grenthe, I. *J. Am. Chem. Soc.* **2001**, *123*, 11999−12008.
(8) Bolvin, H.; Wahlgren, U.; Moll, H.; Reich, T.; Geipel, G.; Fanghänel, Th.; Grenthe, I. *J. Phys. Chem. A* **2001**, *105*, 11441−11445.
(9) Vallet, V.; Wahlgren, U.; Schimmelpfennig, B.; Moll, H.; Szabó, Z.; Grenthe, I. *Inorg. Chem.* **2001**, *40*, 3516−3525.
(10) Wang, Q.; Pitzer, R. M. *J. Phys. Chem. A* **2001**, *105*, 8370−8375.
(11) Tsushima, S.; Reich, T. *Chem. Phys. Lett.* **2001**, *347*, 127−132.
(12) Oda, Y.; Aoshima, A. *J. Nucl. Sci. Technol.* **2002**, *39*, 647−654.
(13) Vallet, V.; Wahlgren, U.; Szabó, Z.; Grenthe, I. *Inorg. Chem.* **2002**, *41*, 5626−5633.
(14) Fuchs, M. S. K.; Shor, A. M.; Rösch, N. *Int. J. Quantum Chem.* **2002**, *86*, 487−501.
(15) García-Hernández, M.; Lauterbach, C.; Fuchs-Rohr, M. S. K.; Krüger, S.; Rösch, N. To be published.
(16) Privalov, T.; Schimmelpfennig, B.; Wahlgren, U.; Grenthe, I. *J. Phys. Chem. A* **2003**, *107*, 587−592.

10.1021/ic035450h CCC: $27.50
Published on Web 06/04/2004

stabilization energies of solvated AnO_2^{2+} (An = U and/or Np, Pu)[1−8] and AnO_2^{+} species.[4] We also mention the recent work of our group on the complexes[15] AnO_2^{2+} (An = U, Np) with water and other small inorganic ligands, employing a combination strategy on the basis of explicit water ligands and the COSMO (conductor-like screening model) solvation model.[14,19]

The redox chemistry of actinides is important to understanding and controlling radionuclide transport, because precipitation, sorption, and colloid formation behavior differ from one oxidation state to another. For example, the vast differences in aqueous solubility between U(VI) and U(IV) species present a possible means to immobilize uranium by converting it into a lower oxidation state. Thus far, only few theoretical studies[4,16−18] have attempted to address the redox properties of actinides. Hay et al.[4] calculated the reduction potentials of the couples $[AnO_2(H_2O)_5]^{2+}/[AnO_2(H_2O)_5]^{+}$ (An = U, Np, Pu) with a hybrid density functional method (B3LYP), combined with a dielectric continuum model, via the adiabatic ionization potentials of the species $[AnO_2(H_2O)_5]^{+}$. These values for the series U, Np, and Pu agreed qualitatively with the experimentally observed trends, but the absolute values were consistently 2−3 eV too large. Privalov et al.[16] undertook an ambitious study of the mechamism for the U(VI) reduction by Fe(II) which corroborated the importance of a proper treatment of solute−solvent interaction. The solvation model was found to alter the reaction energetics with respect to the gas phase by ∼10 kcal/mol at correlated levels; this energy is comparable with the effect of electron correlation on the reaction energy. Vallet et al.[17] proposed a two-step model process for the uranyl reduction by water:

$$UO_2^{2+} + 1/2H_2O \rightarrow UO(OH)^{2+} + 1/4O_2 \qquad (R1)$$

$$UO(OH)^{2+} + 1/2H_2O \rightarrow U(OH)_2^{2+} + 1/4O_2 \qquad (R2)$$

Depending on the method used, Vallet et al.[17] found reaction energies varying from −9.4 to 13.7 kcal/mol for reaction R1 and −0.2 to 5.7 kcal/mol for reaction R2. In their study, density functional (DF) results were compared to those of various Hartree−Fock-based correlated methods; they also examined all-electron methods vs effective core potentials as well as results obtained without and with spin−orbit interaction.[17] DF calculations yielded reaction R1 to be exothermic, at variance with other methods.[17] This benchmark study referred to reactions in the gas phase only. However, for these model reactions to acquire practical relevance, solvent effects in aqueous solution have to be taken into account, as done in the present work.

We employed the same two-step model and examined the effect of solvation on reactions R1 and R2 at three levels of approximation: (i) electrostatic interaction with bulk solvent included via the COSMO approach;[19] (ii) explicit quantum-chemical treatment of the first hydration sphere; (iii) combination of the two preceding models. The change of the reaction free energies due to solvent effects will be shown to be much larger than the scatter between values obtained at different levels of theory for the gas phase.

Computational Methods

All-electron calculations were performed with the linear combination of Gaussian-type orbitals fitting-functions density functional method[20] (LCGTO-FF-DF) as implemented in the parallel code ParaGauss.[21,22] This code permits nonrelativistic as well as relativistic calculations. In this work, the scalar relativistic treatment was chosen because of the heavy-element composition of the chemical systems studied. Spin−orbit effects were neglected; the resulting error in the U(VI) reduction energetics is expected to be 6−7 kcal/mol for each reduction step.[17]

We used two different exchange-correlation functionals: the local-density approximation (LDA) in the parametrization of Vosko, Wilk, and Nusair (VWN);[23] the gradient-corrected functional (generalized gradient approximation, GGA) suggested by Becke and Perdew (BP).[24,25] LDA often yields more accurate results for molecular geometries, whereas gradient-corrected functionals perform better for energy parameters.[26,27] We also refer to results obtained with another GGA exchange-correlation functional, introduced by Perdew, Burke, and Ernzerhof and modified by Hammer and Nørskov (PBEN);[28] it had been successfully applied in our earlier work on the hydration of UO_2^{2+}.[14]

The Kohn−Sham orbitals were represented by flexible Gaussian-type basis sets, contracted in a generalized fashion using atomic eigenvectors of scalar relativistic LDA calculations. For U, we used a basis set of the type (24s, 19p, 16d, 11f), contracted to [10s, 7p, 7d, 4f];[29] O and H atoms were described by standard basis sets,[30] (9s, 5p, 1d) → [5s, 4p, 1d] and (6s, 1p) → [4s,1p], respectively.

Solvation effects were taken into account using the COSMO method implemented in ParaGauss.[14] In the COSMO approach, as in all continuum models (CM), the solute is placed in an empty cavity of a dielectric medium; however, the dielectric outside the cavity is first replaced by a conductor, which allows for a more efficient solution of the electrostatic problem. To adjust for the appropriate dielectric medium, an empirical factor is introduced.[19]

(17) Vallet, V.; Schimmelpfenning, B.; Maron, L.; Teichteil, C.; Leininger, T.; Gropen, O.; Grenthe, I.; Wahlgren, U. *Chem. Phys.* **1999**, *244*, 185−193.

(18) Vallet, V.; Maron, L.; Schimmelpfenning, B.; Leininger, T.; Teichteil, C.; Gropen, O.; Grenthe, I.; Wahlgren, U. *J. Phys. Chem. A* **1999**, *103*, 9285−9289.

(19) Klamt, A.; Schüürmann, G. *J. Chem. Soc., Perkin Trans.* **1993**, *105*, 799−805.

(20) Dunlap, B. I.; Rösch, N. *Adv. Quantum Chem.* **1990**, *21*, 317−339.

(21) Belling, T.; Grauschopf, T.; Krüger, S.; Nörtemann, F.; Staufer, M.; Mayer, M.; Nasluzov, V. A.; Birkenheuer, U.; Hu, A.; Matveev, A. V.; Fuchs-Rohr, M. S. K.; Shor, A. M.; Neyman, K. M.; Ganyushin, D. I.; Rösch, N. *ParaGauss*, version 2.2; Technische Universität München: Munich, Germany, 2001.

(22) Belling, T.; Grauschopf, T.; Krüger, S.; Mayer, M.; Nörtemann, F.; Staufer, M.; Zenger, C.; Rösch, N. In *High Performance Scientific and Engineering Computing*, *Lecture Notes in Computational Science and Engineering*; Bungartz, H.-J., Durst, F., Zenger, C., Eds.; Springer: Heidelberg, Germany, 1999; Vol. 8, pp 439−453.

(23) Vosko, S. H.; Wilk, L.; Nusair, M. *Can. J. Chem.* **1980**, *58*, 1200−1211.

(24) Becke, A. D. *Phys. Rev. A* **1988**, *38*, 3098−3100.

(25) Perdew, J. P. *Phys. Rev. B* **1986**, *33*, 8822−8824; **1986**, *34*, 7406.

(26) Görling, A.; Trickey, S. B.; Gisdakis, P.; Rösch, N. In *Organometallic Chemistry*; Brown, J., Hofmann, P., Eds.; Springer: Heidelberg, Germany, 1999; Vol. 4, pp 109−165.

(27) Koch, W.; Holthausen, M. C. *A Chemist's Guide to Density Functional Theory*, 2nd ed.; Wiley-VCH: Weinheim, Germany, 2000.

(28) Hammer, B.; Hansen, L. B.; Nørskov, J. K. *Phys. Rev. B* **1999**, *59*, 7413−7421.

(29) Minami, T.; Matsuoka, O. *Theor. Chim. Acta* **1995**, *90*, 27−39.

(30) Poirier, R.; Kari, R.; Csizimadia, I. G. *Handbook of Gaussian Basis Sets*; Elsevier: Amsterdam, 1985.

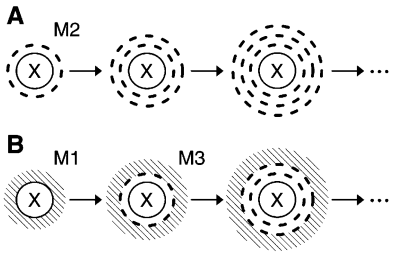

Figure 1. Schematic representation of the two approaches to describe solvation of a solute/ion X. The solute/ion is always described quantum-mechanically. In the first approach (A), solvent molecules (represented by dashes) are included in the quantum-mechanical model; models become more accurate by accounting for an increasing number of solvent shells. The second approach (B), takes long-range electrostatic interactions into account via a polarizable continuum model (CM). The most simple variant M1 includes only a CM treatment of the solute X. More accurate models result from treating a model of type A as the quantum mechanics part of a model of type B; e.g., model M2 with one explicit solvation shell treated with CM yields model M3.

Following the generally adopted classification of continuum models,[31] the COSMO method belongs to the group of apparent surface charge approaches. In addition to the original COSMO model, the ParaGauss solvent module also includes averaged short-range solvent effects via a force field.[14]

The solute cavity for the electrostatic part of the solute−solvent interaction was constructed using atomic spheres of van der Waals radii[32] scaled by 1.2 (except for H). Additional spheres were created according to the GEOPOL algorithm.[33,34] The dielectric constant of water was taken as $\epsilon = 78.39$.

Geometries were first optimized with the VWN functional; then, single-point energies were calculated by applying the CM and the gradient-corrected BP functional. This combination strategy takes advantage of the accuracy of LDA structures but provides improved energy data from the GGA approximation and the environment model.

Results and Discussion

The theoretical description of the solvation of a molecule presents a challenging task because both local interactions (sometimes incorporating chemical interactions of solvent and solute) and bulk effects have to be accounted for. One may aim at a purely quantum-mechanical description of the solvated system, based on a supermolecule approach (Figure 1A).[35] The system size should be large enough to include several solvation shells before convergence of the solvation free energy or other property of interest can be approached; thus, such a strategy is prohibitively expensive for heavy-element complexes. Nevertheless, inclusion of only the first solvation shell often gives a good first-order approximation because it may already cover significant chemical aspects of solvation.

On the other extreme are continuum models (CM) which totally neglect microscopic properties of the solvent.[31] A CM approach allows one to describe electrostatic interactions with the medium by representing the solvent as an unbounded dielectric continuum. While they account for long-range effects, conventional continuum models (see M1 in Figure 1B) have the significant limitation that they exclude chemical interactions between solvent and solute on the molecular level.

As a reasonable compromise, a combination model was recommended,[36] in which one or more solvation shells are treated quantum-mechanically, while the long-range electrostatic effects are accounted for with a continuum model. This strategy is pictorially illustrated in Figure 1B. In practice, it has been common to include only the first solvation shell; in this way one compromises between the computational cost and the accuracy of the model.

In this work, we used and compared three levels of approximation to incorporate solvent effects (Figure 1): (M1) description of long-range interactions via the continuum model COSMO; (M2) explicit quantum-chemical treatment of the first hydration sphere, i.e., complexes $[UO_2(H_2O)_n]^{2+}$, $[UO(OH)(H_2O)_n]^{2+}$, and $[U(OH)_2(H_2O)_n]^{2+}$ ($n = 4-6$) were considered without further reference to the solvent; (M3) explicit quantum-chemical treatment of the first hydration sphere, while further coordination shells are implicitly incorporated via the continuum model. Recently, we demonstrated the performance of the COSMO model for the solvation of uranyl,[14] where LDA and GGA (PBEN[28]) geometries for hydrated uranyl were shown to be in very good agreement with available experimental data when the first hydration shell was explicitly included in the model. Free energies of uranyl hydration calculated with an approach of type M3 agreed well with experiment.[14]

In the following, we first focus on the structural and electronic properties of the hydrated species UO_2^{2+}, $UO(OH)^{2+}$, and $U(OH)_2^{2+}$, including their hydration energies. Then we will discuss the energetics of reactions R1 and R2 and compare them to those obtained in an earlier study.[17]

Properties of Aquo Complexes. (a) Geometries. The optimized geometries of the complexes $[UO_2(H_2O)_n]^{2+}$, $[UO(OH)(H_2O)_n]^{2+}$, and $[U(OH)_2(H_2O)_n]^{2+}$ ($n = 0, 4-6$) are summarized in Table 1. The definitions of the geometrical parameters are shown in Figure 2. First, we optimized nonligated species, i.e., complexes with $n = 0$ (for these linear species, the point groups D_{5h} or C_{5v} were assumed); then, the aquo ligands were attached to the actinide center in the equatorial plane. Whereas the linearity of the OUO moiety of $[UO_2(H_2O)_n]^{2+}$ is well established, we found by unconstrained optimization that $UO(OH)^{2+}$ and $U(OH)_2^{2+}$ are also linear with both the LDA (VWN) and the GGA (BP) exchange-correlation approximations. Apparently, the interaction of an H(1s) orbital with the σ_u HOMO orbital of UO_2^{2+} is optimal in the linear geometry. Inclusion of the interactions with the solvent via the CM did not affect the linearity of these ions. Interestingly, Hay et al.[4] found a linear U−O−H fragment in the complex $[UO_2(H_2O)_4(OH)]^+$, contrary to the intuitive expectation of a bent structure (like H−O−H in H_2O) and in contrast to the di- and tetrahydroxo

(31) Tomasi, J.; Persico, M. *Chem. Rev.* **1994**, *94*, 2027−2049.
(32) Bondi, A. *J. Phys. Chem.* **1964**, *68*, 441−451.
(33) Pasqual-Ahuir, J. L.; Silla, E. *J. Comput. Chem.* **1990**, *11*, 1047−1060.
(34) Silla, E.; Tuñón, I.; Pasqual-Ahuir, J. L. *J. Comput. Chem.* **1991**, *12*, 1077−1088.
(35) Gao, J. *Rev. Comput. Chem.* **1995**, *7*, 119−185.
(36) Miertus, S.; Scrocco, E.; Tomasi, J. *Chem. Phys.* **1981**, *55*, 117−129.

Table 1. Calculated Structural Parameters[a] of U(VI, V, VI) Complexes without and with Various Numbers of Aquo Ligands and Comparison with Experiment

	method	$d1_{U-O}$	$d2_{U-O}$	$d3_{U-O}$	$d1_{O-H}$	$d2_{O-H}$	$\alpha1_{O-U-O}$	$\alpha2_{O-U-O}$	α_{H-O-H}
UO_2^{2+}	VWN	1.705						180.0	
$[UO_2(H_2O)_4]^{2+}$	VWN	1.756		2.359		0.984	90.0	180.0	107.9
$[UO_2(H_2O)_5]^{2+}$, D_{5h}	VWN	1.760		2.417		0.980	90.0	180.0	107.8
$[UO_2(H_2O)_5]^{2+}$, C_s	VWN	1.764, 1.765		2.410, 2.386, 2.460		0.981	90.2, 78.4, 112.7	171.4	108.2, 108.3, 108.3
$[UO_2(H_2O)_6]^{2+}$, D_{6h}	VWN	1.757		2.528		0.977	90.0	180.0	107.9
$[UO_2(H_2O)_6]^{2+}$, D_{3d}	VWN	1.774		2.447		0.979	72.5	180.0	109.0
UO_2^{2+}	VWN + CM[b]	1.718					90.0	180.0	
UO_2^{2+}(aq), expt[c]		1.76		2.41				180.0	
UO_2^{2+}(aq), expt[d]		1.78		2.41				180.0	
$UO(OH)^{2+}$	VWN	1.715	1.883		1.008			180.0	
$[UO(OH)(H_2O)_4]^{2+}$	VWN	1.777	1.972	2.372	0.985	0.983	92.3	180.0	107.6
$[UO(OH)(H_2O)_5]^{2+}$, C_{5v}	VWN	1.783	1.979	2.427	0.983	0.980	92.2	180.0	107.5
$[UO(OH)(H_2O)_5]^{2+}$, C_s	VWN	1.785	1.980	2.425, 2.444, 2.425	0.983	0.980	101.0, 81.7, 101.0	176.9	107.8, 108.1, 107.6
$[UO(OH)(H_2O)_6]^{2+}$, C_{6v}	VWN	1.780	1.978	2.541	0.983	0.977	91.6	180.0	107.5
$[UO(OH)(H_2O)_6]^{2+}$, C_{3v}	VWN	1.801	2.007	2.468, 2.465	0.980	0.978, 0.979	74.2, 107.6	180.0	108.5, 109.1
$UO(OH)^{2+}$	VWN + CM[b]	1.743	1.884		0.996			180.0	
$U(OH)_2^{2+}$	VWN		1.925		1.000		90.0	180.0	
$[U(OH)_2(H_2O)_4]^{2+}$	VWN		2.019	2.383	0.982	0.982	90.0	180.0	107.9
$[U(OH)_2(H_2O)_5]^{2+}$, D_{5h}	VWN		2.030	2.439	0.980	0.979	90.0	180.0	107.6
$[U(OH)_2(H_2O)_5]^{2+}$, C_s	VWN		2.031, 2.032	2.412, 2.432, 2.514	0.980	0.980, 0.979	87.9	166.5	108.2, 108.0, 108.0
$[U(OH)_2(H_2O)_6]^{2+}$, D_{6h}	VWN		2.030	2.554	0.980	0.976	90.0	180.0	107.5
$[U(OH)_2(H_2O)_6]^{2+}$, D_{3d}	VWN		2.064	2.472	0.977	0.9770.978	72.9	180.0	111.8
$U(OH)_2^{2+}$	VWN + CM[b]		1.963		0.987		90.0	180.0	
H_2O	VWN					0.972			

[a] See Figure 2 for definitions; distances in Å and angles in deg. [b] CM was self-consistently applied in geometry optimization. [c] Reference 40. [d] Reference 5.

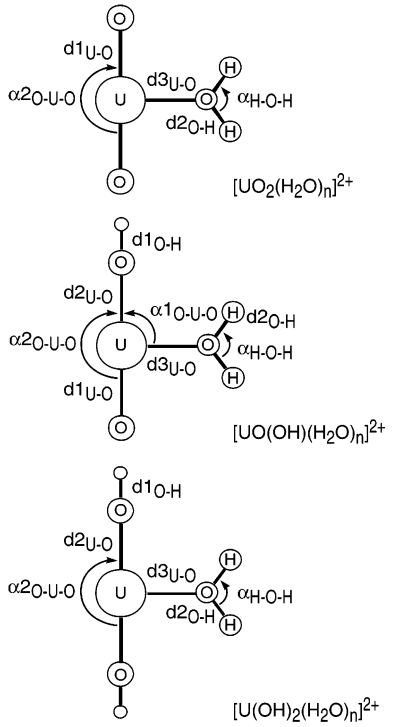

Figure 2. Definition of the structural parameters of the complexes $[UO_2(H_2O)_n]^{2+}$, $[UO(OH)(H_2O)_n]^{2+}$, and $[U(OH)_2(H_2O)_n]^{2+}$.

complexes, $[UO_2(OH)_2]$ and $[UO_2(OH)_4]^{2-}$, where bent U−O−H fragments were predicted[5,37−39] theoretically.

Reliable experimental geometries are available only for aqueous UO_2^{2+} (Table 1). The U−O bond length calculated in the gas-phase approximation using the VWN functional, 1.705 Å, is 0.05−0.07 Å shorter than experimental values measured for hydrated UO_2^{2+}, 1.76 and 1.78 Å.[5,40] Vallet et al.[17] obtained 1.706 and 1.711 Å for gas-phase UO_2^{2+} in CCSD(T) and ACPF calculations. The corresponding PBEN result[14] for U−O bond in the nonhydrated uranyl, 1.723 Å, is slightly larger than these values. When solvation was included via strategy M3 (explicit water ligands, coordinated to uranyl, combined with CM), both the VWN and PBEN methods furnished the U−O bond length in excellent agreement with experiment, 1.765 and 1.772 Å, respectively.[14] The equatorial U−O distances in $[UO_2(H_2O)_5]^{2+}$, computed with the VWN functional, with and without CM, were 2.468[14] and 2.417 Å, respectively. The latter value is close to the experimental result, 2.41 Å.[5,40] The corresponding PBEN distances with and without CM, 2.639[14] and 2.530 Å,[14] respectively, are notably longer. Geometrical parameters calculated with another gradient-corrected functional (BLYP) were close to the PBEN values: the axial UO distance was calculated at 1.803 Å, and the equatorial UO distance, at 2.516 Å.[4] As expected, LDA calculations provide more accurate equilibrium geometries than GGA calculations.

As the oxidation state changes from VI to IV, the axial U−O distances increase (Table 1). This mainly concerns the U−O(H) bonds (denoted $d2_{U-O}$ in Table 1), which increase by 0.17 Å going from UO_2^{2+} to $UO(OH)^{2+}$ and by 0.22 Å from UO_2^{2+} to $U(OH)_2^{2+}$. The terminal UO bond, $d1_{U-O}$, also elongates by 0.01 Å upon addition of a hydrogen atom (Table 1).

The Mulliken charge of the uranium center increases only slightly in the sequence UO_2^{2+}, $UO(OH)^{2+}$, and $U(OH)_2^{2+}$, from 1.99 to 2.04 e, at variance with the trend of the formal oxidation state of U, which changes from +6 to +4. There

(37) Privalov, T.; Schimmelpfennig, B.; Wahlgren, U.; Grenthe, I. *J. Phys. Chem. A* **2002**, *106*, 11277−11282.
(38) Schreckenbach, G.; Hay, P. J.; Martin, R. L. *J. Comput. Chem.* **1999**, *20*, 70−90.
(39) Schreckenbach, G.; Hay, P. J.; Martin, R. L. *Inorg. Chem.* **1998**, *37*, 4442−4451.
(40) Allen, P. G.; Bucher, J. J.; Shuh, D. K.; Edelstein, N. M.; Reich, T. *Inorg. Chem.* **1997**, *36*, 4676−4683.

Table 2. Solvation Free Energies and Gas-Phase Binding Energies[a] (kcal/mol) of Uranium Species, Calculated at the BP Level[b]

	$\Delta E^{(g)}_{binding,0}$	ΔG^{CM}_{298}	$-n\Delta G^{CM}_{298}(H_2O)$	$\Delta G^{sol,total}_{298}$	ΔG^{M3-M1}
UO_2^{2+}		−297[c]			
$[UO_2(H_2O)_4]^{2+}$	−237 (−59), −233,[d] −214[e]				−123[d]
$[UO_2(H_2O)_5]^{2+}$, D_{5h}	−263 (−53), −257,[d] −243,[e] −353[f]	−193, −188[d]	34	−421	−125, −130,[d] −58.3[f]
$[UO_2(H_2O)_5]^{2+}$, C_s	−264 (−53)	−192	34	−422	−125
$[UO_2(H_2O)_6]^{2+}$, D_{6h}	−258 (−43), −253,[d] −241,[e] −350[f]	−184	41	−402	−105, −112,[d] −34.8[f]
$[UO_2(H_2O)_6]^{2+}$, D_{3d}	−280 (−47)	−184	41	−423	−126
$UO(OH)^{2+}$		−282[c]			
$[UO(OH)(H_2O)_4]^{2+}$	−213 (−53)				
$[UO(OH)(H_2O)_5]^{2+}$, C_{5v}	−228 (−46)	−187	34	−381	−99
$[UO(OH)(H_2O)_5]^{2+}$, C_s	−235 (−47)	−188	34	−388	−106
$[UO(OH)(H_2O)_6]^{2+}$, C_{6v}	−223 (−37)	−177	41	−359	−77
$[UO(OH)(H_2O)_6]^{2+}$, C_{3v}	−242 (−40)	−179	41	−380	−98
$U(OH)_2^{2+}$		−257[c]			
$[U(OH)_2(H_2O)_4]^{2+}$	−201 (−50)				
$[U(OH)_2(H_2O)_5]^{2+}$, D_{5h}	−222 (−44)	−180	34	−368	−112
$[U(OH)_2(H_2O)_5]^{2+}$, C_s	−224 (−45)	−180	34	−370	−113
$[U(OH)_2(H_2O)_6]^{2+}$, D_{6h}	−217 (−36)	−172	41	−348	−91
$[U(OH)_2(H_2O)_6]^{2+}$, D_{3d}	−233 (−39)	−174	41	−366	−109

[a] $\Delta E^{(g)}_{binding,0}$ = gas-phase binding energy (M2); binding energies/ligand are given in parentheses. ΔG^{CM}_{298} = CM increment to the hydration free energy. $-n\Delta G^{CM}_{298}(H_2O)$ = same quantity for n water molecules. $\Delta G^{sol,total}_{298}$ = total hydration free energy (M3) as sum of the preceding three columns. ΔG^{M3-M1} = defect of the CM treatment as defined by eq 3. [b] Single-point calculations performed on the geometries optimized at the VWN level. BP + CM energies were calculated only for $n = 5$ and 6. [c] Corresponding to free energy of hydration by model M1. [d] Reference 1. [e] Reference 6. [f] Reference 3.

is no contradiction, because the U−O bonds are in fact covalent and the electronegativities of O and OH are quite close, both around 3.5,[41] so that both electron-acceptor groups are expected to draw about the same amount of electron density, leaving the charge of ∼+2e on the U atom.

It is informative to inspect the structural changes resulting from the different solvation models. As seen from Table 1, optimization of the geometries with the simple CM (without explicit consideration of H_2O molecules; M1) increases the UO bond length by about 0.01 Å. The UO bonds in $UO(OH)^{2+}$ and $U(OH)_2^{2+}$ also elongate. The positive charge of the uranium center increases due to solvation, which polarizes the bonds; however, as we will see below, this is not the case when explicit water ligands are considered.

When optimizing complexes with water ligands coordinated to the U atom, we first imposed D_{nh} or C_{nv} ($n = 4-6$) constraints (referred to as "high-symmetry" structures) and then studied the effect of symmetry lowering for $n = 5$ and 6. In the high-symmetry complexes, water ligands were arranged in the equatorial plane of the linear solute unit with the H−O−H planes oriented perpendicular to that plane. Earlier studies on pentaaquo uranyl[4,6] found the D_{5h} structure of $[UO_2(H_2O)_5]^{2+}$ to be less than 1 kcal/mol above the true minimum. However, our own studies showed that, for complexes with six H_2O ligands, symmetry lowering resulted in a significant structure relaxation and stabilization.

Compared to nonsolvated UO_2^{2+}, $UO(OH)^{2+}$, and $U(OH)_2^{2+}$, the axial UO distances increased in the hydrated species, whereas the axial OH bond distances decreased slightly. Uranium bonding with equatorial ligands competes with the bonding between U and axial oxygen centers. Looking at the geometries of the "high-symmetry" hydrates, one observes that as the number of aquo ligands increases from 4 to 6, the equatorial U−O distances increase monotonically and the binding energies/ligand decrease (Table 2), whereas the axial UO distances go through a maximum at $n = 5$. This observation lead us to suspect that, for $n = 6$, the destabilization caused by van der Waals repulsion between aquo ligands is stronger than the stabilization due to addition of one more H_2O molecule. Indeed, for $n = 6$, the distances between equatorial oxygen centers, ∼2.5 Å, are 0.4 Å shorter than twice the van der Waals radius of an O atom (2.9 Å),[32] whereas, for $n = 5$, the corresponding inter-oxygen distance is 2.84 Å in $UO_2(H_2O)_5^{2+}$, or slightly longer in $[UO(OH)(H_2O)_5]^{2+}$ and $[U(OH)_2(H_2O)_5]^{2+}$, hence at the border. To examine the consequences in more detail, we reoptimized complexes with $n = 6$, reducing the symmetry to D_{3d} and C_3 point groups instead of D_{6h} and D_{3d}, to allow oxygen atoms of aquo ligands to move out of the equatorial plane. Such geometry relaxation was found to reduce the total energy by 21−27 kcal/mol at the VWN level; the corresponding gas-phase BP binding energies (first column of Table 3) were reduced by 16−22 kcal/mol. Due to this structural relaxation, the equatorial U−O bond distances shrank by about 0.1 Å whereas the axial U−O bonds elongated by 0.02−0.04 Å (Table 1).

Therefore, we investigated lower-symmetry conformers of the pentaaquo complexes as well but found less significant energy lowering of 2−5 kcal/mol for C_5, C_s, and C_1 structures

Table 3. Solvation Energies[a] of UO_2^{2+}, $UO(OH)^{2+}$, and $U(OH)_2^{2+}$ Determined from the Models M1−M3 at the BP Level[b]

	M1	M2[c]	M3[c]	expt
UO_2^{2+}	−297	−264	−422	-297 ± 5,[d] $-437 \le \Delta_h G^\circ \le -318$[e]
$UO(OH)^{2+}$	−282	−235	−388	
$U(OH)_2^{2+}$	−257	−224	−370	

[a] Models M1−M3 are described in the text. Experimentally based estimates for the free energy of hydration of uranyl are also shown. [b] Single-point calculations performed on the geometries optimized at the VWN level. [c] Values calculated for $[X(H_2O)_5]^{2+}$. [d] Estimated using $\Delta_f H^\circ(UO_2^{2+}) = 289 \pm 5$ kcal/mol.[51,53] [e] Estimated using $\Delta_f H^\circ(UO_2^{2+}) = 311 \le \Delta_f H^\circ \le 430$ kcal/mol.[62]

(41) The electronegativity of an OH group was estimated to ∼3.5 kcal/mol by various methods; for more information, see the following: Wells, P. R. In *Progress in Physical Organic Chemistry*; Taft, R. W., Ed.; Academic: New York, 1968; Vol. 6, pp 111−145.

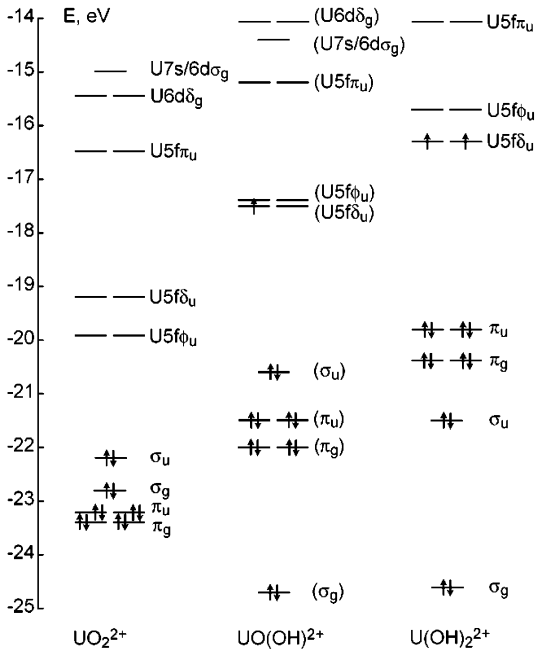

Figure 3. Schematic sequence of the valence orbital energies near the HOMO−LUMO gap of the three complexes UO_2^{2+}, $UO(OH)^{2+}$, and $U(OH)_2^{2+}$. For $UO(OH)^{2+}$, the orbital notations are taken in parentheses, because these irreducible representation notations correspond to the group $D_{\infty h}$ and, strictly speaking, do not apply to $UO(OH)^{2+}$.

at the VWN level. The total free energies of hydration for $UO_2(H_2O)_5^{2+}$ and $[U(OH)_2(H_2O)_5]^{2+}$ were essentially not affected, whereas the total free energy of hydration of $[UO(OH)(H_2O)_5]^{2+}$ was reduced by 7 kcal/mol. Tables 2 and 3 list only the results for the complexes at D_{5h}/C_{5v} symmetry and the lowest energy C_s conformers; the geometry and energetics of the other pentacoordinated structures explored can be found in the Supporting Information.

(b) Electronic Structure. UO_2^{2+} is a closed-shell species, $^1\Sigma_g^+$, with a formal $5f^0$ configuration of uranium. For some time, the electronic structure of uranyl was the subject of extensive discussions.[42,43] The most controversial issues concerned the phenomenon of UO_2^{2+} linearity as opposed to the isoelectronic bent ThO_2.[42,43] It was established that the highest occupied orbitals of UO_2^{2+} comprise a set of orbitals σ_g, σ_u, π_g, and π_u (Figure 3). This work concurs with that analysis:[42] at both the VWN or BP level, the relative ordering obtained is $\pi_g < \pi_u < \sigma_g < \sigma_u$ (Figure 3). In this set, π_u and σ_u exhibit significant U 5f−O 2p bonding character, and π_g is a U 6d−O 2p bonding orbital. The lowest virtual orbitals have strong U 5f character; the ordering of the U 5f manifold agrees with that given in a recent experimental study:[44] U 5f$\phi \approx$ U 5f$\delta <$ U 5f$\pi_u^* \ll$ U 5fσ_u^*. The U 5fσ_u^* orbital is involved in U−O bonding, hence displaced to higher energies; some U 6d orbitals follow the U 5fπ_u^* level immediately at higher energies. The lowest lying virtual U5f orbitals are two degenerate pairs, U 5fδ and U 5fϕ, of essentially atomic character, which by symmetry cannot mix with any filled orbital of oxygen.

Addition of a hydrogen atom to one of the uranyl oxygen centers can be formally viewed as donation of one of the oxygen lone pairs to the H atom and a promotion of an extra electron to the lowest 5f orbital of U in $UOOH^{2+}$, 5fδ. This is essentially what we see from the population analysis. The former σ_g orbital of uranyl, which was mainly localized on the O atoms, acquires O−H bonding character in $UO(OH)^{2+}$. This orbital hence moves down in energy, by 1.9 eV, below π_u and π_g, while π_u in turn rises in energy, by 1.7 eV, due to reduced participation of the 5f orbitals (Figure 3). The unpaired electron occupies the U5fδ orbital, to give a $^2\Delta$ electronic state at variance with Vallet et al.,[17] who found the U 5fϕ orbital to be below the U 5fδ and reported a $^2\Phi$ ground state for this species. Actually, the 5fδ and 5fϕ orbitals are nearly degenerate and will mix if spin−orbit interaction is considered. The more precise spin−orbit treatment[4,45,46] of the isoelectronic NpO_2^{2+} predicts a $(\delta_u,\phi_u)^1$ configuration for the lowest electronic states with $\Omega = 5/2$ (a mixture of $^2\Phi_{5/2u}$ and $^2\Delta_{5/2u}$, with a larger contribution by the former state) and $\Omega = 3/2$ ($^2\Delta_{3/2u}$) at a slightly higher energy, in agreement with experiment.[47]

Another issue, related to partially filled degenerate orbitals, is the Renner−Teller effect. At first glance, it seems a bit surprising that $UO(OH)^{2+}$ favors a linear geometry, because molecules with partially occupied degenerate shells tend to undergo a structure change that removes the degeneracy.[48] Note also the linear geometry of the isoelectronic species UO_2^+. The fact that the 5f orbitals of U have an essentially atomic character plays a crucial role here, as well as the stabilizing effect of the interaction U 5f−O 2p, strongly favoring a linear geometry.

The change in electronic structure upon going from $UO(OH)^{2+}$ to $U(OH)_2^{2+}$ is quite obvious in the light of the preceding discussion. In our scalar-relativistic picture, the additional electron ends up in the U 5fδ orbital to yield a δ^2 configuration corresponding to the $^3\Sigma_g^-$ state, again at variance with the MRCI treatment of Vallet et al.,[17] who report a $\phi^1\delta^1$ configuration and a ^3H_g ground state. In our single-determinant approach the $\phi^1\delta^1$ state was 0.3 eV higher; clearly, the MRCI treatment is more appropriate for such a multiplet. Spin−orbit CI calculations[4,45,49] for isoelectronic NpO_2^+ and PuO_2^{2+} predicted a $^3H_{4g}$ ($\phi^1\delta^1$) ground state, which agrees with results of polarized single-crystal adsorption spectroscopy[47] and EPR[50] studies. On the other hand, scalar-relativistic DF calculations[4] for these species yielded the state $^3\Sigma_g^-$ in agreement with our results. In $U(OH)_2^{2+}$, the ordering of the four highest filled orbitals changes again,

(42) Pepper, M.; Burstein, B. E. *Chem. Rev.* **1991**, *91*, 719−741.
(43) Dyall, K. *Mol. Phys.* **1999**, *96*, 511−518.
(44) Denning, R. G.; Green, J. G.; Hutchings, T. E.; Dallera, C.; Tagliaferri, A.; Giarda, K.; Brookes, N. B.; Braicovich, L. *J. Chem. Phys.* **2002**, *117*, 8008−8020.
(45) Matsika, S.; Pitzer, R. M. *J. Phys. Chem. A* **2000**, *104*, 4064−4068.
(46) Matsika, S.; Zhang, Z.; Brozell, S. R.; Blaudeau, J.-P.; Wang, Q.; Pitzer, R. M. *J. Phys. Chem. A* **2001**, *105*, 3825−3828.
(47) Denning, R. G.; Norris, J. O. W.; Brown, D. *Mol. Phys.* **1982**, *46*, 287−323; 325−364.
(48) Albright, Th. A.; Burdett, J. K.; Whangbo M.-H. *Orbital Interactions in Chemistry*; Wiley: New York, 1985.
(49) Maron, M.; Leininger, T.; Schimmelpfennig, B.; Vallet, V.; Heully, J.-L.; Teichteil, C.; Gropen, O.; Wahlgren, U. *Chem. Phys.* **1999**, *244*, 195−201.
(50) Bleaney, R. G. *Discuss. Faraday Soc.* **1955**, *19*, 112−118.

and the σ_u orbital also shifts down below π_g due to the bonding interaction with the σ_u H based combination (Figure 3): $\sigma_g < \sigma_u < \pi_g < \pi_u$. The π_g and π_u orbitals maintain their character (U 6d−O 2p and U 5f−O 2p, respectively) although the contribution of uranium is significantly weakened compared to UO_2^{2+}, especially that of the U 5f orbitals, which overlap much less as the U−O bond length increases.

The influence of solvation on the molecular orbitals is quite similar for all three species. The straightforward CM does not affect the orbital ordering, whereas the contributions from the U 5f and 6d orbitals decrease due to increased U−O bond distances. Coordination of aquo ligands to uranium has a more pronounced effect. First of all, π_g and π_u [or their counterparts in $UO(OH)^{2+}$] are slightly destabilized, so that, in $[UO_2(H_2O)_n]^{2+}$, the π_u orbital rises above the σ_g orbital. Noninteracting lone pairs on the aquo oxygen centers introduce several nonbonding orbitals whose energies are close to the HOMO, and for $[UO_2(H_2O)_n]^{2+}$ ($n = 5, 6$), such a lone pair replaces the HOMO. Another set of lone pairs (those which interact with the uranium atom) form a lower lying group of occupied levels with small contributions of U 5f and 6d orbitals; thus, they compete with axial π-bonding. Nevertheless, solvation leaves the gross features of the electronic structure unchanged in all cases.

Energetics. We start this section with the discussion of the solvation energies of the uranium species under study. The solvation Gibbs free energy of UO_2^{2+} was calculated earlier;[14] experimental estimates of the hydration enthalpy[51,52] and the hydration free energy[51,53] are also available. It should be informative, on one hand, to compare the results of the current approaches with earlier results and with experiment. On the other hand, in the present context it is obvious to examine how the solvation energy depends on the oxidation state and (where appropriate) on the number of H_2O molecules included explicitly in the first solvation shell. Afterward, we will discuss the redox energetics in solution, which in turn is directly affected by differences in the solvation energies of the oxidized and reduced forms.

Solvation Energies. We calculated the solvation energies of uranyl and its reduced species by the three approaches outlined above: M1−M3. First, we shall describe these models in a consistent manner giving all necessary equations and showing the thermodynamic relationships between the solvation free energies calculated by M1−M3. In this work, we applied certain approximations and we will comment on them as we proceed.

M1. In model M1, a CM was applied to bare ions (i.e. without explicit treatment of the first solvation shell). Schematically, model M1 is described by reaction R3:

$$X(g) \rightarrow X(aq,CM) \qquad (R3)$$

Here X = UO_2^{2+}, $UOOH^{2+}$, and $U(OH)_2^{2+}$.

The notation "(aq,CM)" indicates here and further the description of solvation that takes into account only long-range electrostatic effects. The free energies of hydration obtained by this method are listed in Table 2 as ΔG^{CM}_{298}.

M2. The second approach to the description of the interaction with the solvent was, as discussed earlier, a completely quantum-chemical explicit solvation model, in which the free energy of hydration was approximated by the energy change of reaction R4 in the gas phase at 0 K:

$$X(g) + nH_2O(g) \rightarrow [X(H_2O)_n](g) \qquad (R4)$$

In other words, this energy is the gas-phase binding energy of n water molecules to X, $\Delta E^{(g)}_{binding,0}$. Note the difference between $\Delta E^{(g)}_{binding,0}$ and the free energy change of (R4), $\Delta G^{(g)}_{298}$. At room temperature

$$\Delta G^{(g)}_{298} = \Delta E^{(g)}_{binding,0} + \Delta^* \qquad (1)$$

where Δ^* includes the change of the zero point energy ΔZPE and thermal corrections, which comprise electronic, vibrational, rotational, and translational thermal contributions to the internal energy as well as the terms ΔnRT and $-T\Delta S$.[54] Δ^* is substantial and amounts to about 10 kcal/mol per water ligand.[4,55] Therefore, this term should not be ignored in a comparison with experiment. However, in this work, Δ^* was neglected, because in the redox reactions discussed later the corresponding corrections are estimated to be much smaller since they essentially cancel.

M3. In a combination approach, which couples the explicit consideration of the first solvation shell with a CM treatment of the remaining solvent, the free energy of solvation is determined as the approximate free energy change $\Delta G^{sol,total}_{298}$ of reaction R5:

$$X(g) + nH_2O(aq,CM) \rightarrow [X(H_2O)_n](aq,cm) \qquad (R5)$$

Here, the continuum model is applied to both the water molecules on the left-hand side and the hydrated species $[X(H_2O)_n]$ on the right-hand side of the equation. Comparison of reactions R4 and R5 makes it evident that

$$\Delta G^{sol,total}_{298} = \Delta G^{(g)}_{298} + \Delta G^{CM}_{298}([X(H_2O)_n]) - n\Delta G^{CM}_{298} \qquad (2)$$

where the CM terms are free energies from a continuum model. Our estimate of the solvation free energy of model M3 is an approximation to $\Delta G^{sol,total}_{298}$ up to the missing correction Δ^* of $\Delta G^{(g)}_{298}$, eq 1. We define the defect ΔG^{M3-M1} of the continuum model as the difference between $\Delta G^{sol,total}_{298}$ and $\Delta G^{CM}_{298}(X)$:

$$\Delta G^{M3-M1} = \Delta G^{(g)}_{298} + \Delta G^{CM}_{298}([X(H_2O)_n]) - n\Delta G^{CM}_{298}(H_2O) - \Delta G^{CM}_{298}(X) \qquad (3)$$

(51) Marcus, Y. *J. Inorg. Nucl. Chem.* **1975**, *37*, 493−501.
(52) Denning, R. In *Gmelin Handbook of Inorganic Chemistry*; Springer-Verlag: Berlin, 1983; U Suppl. Vol. A6, p 46.
(53) Marcus, Y. *Ion Solvation*; Wiley & Sons: New York, 1985; p 263.
(54) Hehre, W. J.; Radom, L.; Schleyer, P. v. R.; Pople, J. A. *Ab initio Molecular Orbital Theory*; Wiley: New York, 1986.
(55) Martin, R. L.; Hay, P. J.; Pratt, L. R. *J. Phys. Chem. A* **1998**, *102*, 3565−3573.

This is just the free energy change of the hypothetical reaction R6:

$$X(aq,CM) + nH_2O(aq,CM) \rightarrow [X(H_2O)_n](aq,CM) \quad (R6)$$

Therefore, the quantity ΔG^{M3-M1} [in previous works referred to as "binding energy (aq)"[3] or dissociation energy (liquid)"[1]] accounts for the effects of covalent bonding of ligands and thus provides a measure of the deficiency of the pure CM model. Because of the approximate nature of $\Delta G^{(g)}_{298}$ in this work, the values ΔG^{M3-M1} in Table 2 are expected to be substantially overestimated (in absolute value) by the amount of Δ^* (about 40−50 kcal/mol), just as were the values of ref 1, where the same approximation was made. These corrections would notably reduce the differences with the values of ref 3 where ΔG^{M3-M1} values of −58.3 and −34.8 kcal/mol were calculated for $[UO_2(H_2O)_5]^{2+}$ and $[UO_2(H_2O)_6]^{2+}$, respectively.

Table 2 compares different contributions to $\Delta G^{sol,total}_{298}$, which enter eq 2; note that according to eq 2 the next to last column is the sum of the preceding three columns. Calculated values of $\Delta E^{(g)}_{binding,0}$ for 4−6 aquo ligands to uranyl range from −237 to −280 kcal/mol and underestimate the absolute value of the total solvation energy $\Delta G^{sol,total}_{298}$ by 140−160 kcal/mol. As seen from Table 2, $\Delta G^{CM}_{298}(X)$ ($X = UO_2^{2+}$, $UO(OH)^{2+}$, $U(OH)_2^{2+}$) of nonligated ions (M1) also recovers only a part of the total solvation energy, underestimating its absolute value by some 100 kcal/mol. However, this difference would be significantly smaller if the values for $\Delta G^{sol,total}_{298}$ were corrected by Δ^* (about 40−50 kcal/mol).

We can also compare current results with those of earlier studies[1,3,4,6,14] on uranyl aquo complexes with the strategies M2 (ligated complex) and M3 (ligated complex + CM), although most of these studies did not explicitly specify the solvation energy of $[UO_2(H_2O)_n]^{2+}$. The gas-phase binding energies of refs 1, 3, and 6 are given in Table 2 for comparison. Our values of $\Delta E^{(g)}_{binding,0}$ (M2) agree best with the BLYP results of ref 1; the MP2 values[6] are consistently higher by ∼20 kcal/mol, whereas the B3LYP values of ref 3 are surprisingly too negative, by about 100 kcal/mol. In qualitative agreement with this work (in cases where D_{5h} or D_{6h} symmetry was imposed), these three studies gave very close binding energies for the penta- and hexacoordinated complexes, with a slight preference for the former. In ref 4, the complexes were optimized without symmetry constraints, and in agreement with our reduced symmetry calculations, the hexacoordinated complex was found to be most stable in the gas phase. Although absolute values of $\Delta E^{(g)}_{binding,0}$ were not reported in ref 4, the differences in $\Delta E^{(g)}_{binding,0}$ (without ZPE correction) between 5 and 4 and between 6 and 5 aquo ligands were −29 and −22 kcal/mol, respectively, to be compared with −27 and −16 kcal/mol found in this work.

Tsushima et al.[3] employed the original PCM method[36] to which the present COSMO model is a computationally more efficient alternative. The value of ΔG^{CM}_{298} for $[UO_2(H_2O)_5]^{2+}$, −188 kcal/mol, reported by Tsushima et al.[3], is very close to our result, −193 kcal/mol, although our result for ΔG^{M3-M1}, −125 kcal/mol, is twice as large as their reported value of −58.3 kcal/mol.[3] The gas-phase binding energies $\Delta E^{(g)}_{binding,0}$ of ref 3 differ significantly if one compares them to other theoretical studies[1,6] and this work. Their $\Delta E^{(g)}_{binding,0}$ for $[UO_2(H_2O)_5]^{2+}$, −353 kcal/mol, is much below our value for that complex, −263 kcal/mol. Substitution of the values from ref 3 into eq 2 and assuming $\Delta G^{CM}_{298}(H_2O) = 7$ kcal/mol yields $\Delta G^{sol,total}_{298} = -506$ kcal/mol, more than 100 kcal/mol in absolute value above the current result.

The results of Simpler et al.,[1] who used the BLYP functional and a simple Onsager cavity model,[56] are most consistent with ours in terms of $\Delta E^{(g)}_{binding,0}$ and ΔG^{M3-M1} (Table 2). Although these authors do not explicitly give the total solvation energy, it can be estimated from their data at −427 kcal/mol, using our value for $\Delta G^{CM}_{298}(UO_2^{2+}) = -297$ kcal/mol and eq 3. Alternatively, if one takes their value for $\Delta E^{(g)}_{binding,0}$ and our value of ΔG^{CM}_{298} for $[UO_2(H_2O)_5]^{2+}$, one obtains $\Delta G^{sol,total}_{298} = -416$ kcal/mol using eq 2. In earlier work employing the PBEN functional,[14] our group calculated $\Delta E^{(g)}_{binding,0} = -253$ kcal/mol and $\Delta G^{CM}_{298}([UO_2(H_2O)_5]^{2+}) = -179$ kcal/mol; these values result in $\Delta G^{sol,total}_{298} = -407$ kcal/mol, in overall good agreement with the present results.

Inspection of the results obtained with the models M1−M3 (Table 3) reveals that both the simple CM model M1 and the purely quantum-chemical model M2 significantly underestimate the size of the solvation free energy by ∼100−125 and ∼150 kcal/mol, respectively. Note that the model M1 depends crucially on the choice of the van der Waals radius r_U of the uranium atom. Here, we adopted the value of 1.86 Å;[32] our previous study[14] showed that with $r_U = 1.70$ Å the negative hydration free energy of uranyl becomes 32 kcal/mol more negative. This highlights a severe disadvantage of the model M1 in comparison with other models. Qualitatively, all three models demonstrate that the absolute value of the solvation energy is reduced as the oxidation state changes from VI to IV. The redox energetics (see below) in solution favor uranium species in higher oxidation states. The solvation energies of the three compounds investigated, UO_2^{2+}, $UO(OH)^{2+}$, and $U(OH)_2^{2+}$, are, of course, comparable in size due to the large effect of the total charge of +2 e. Contributions of the dipole and higher multipole moments are 1 order of magnitude smaller, but they differentiate the solvation behavior of the three compounds. The hydrogen-free oxygen centers of UO_2^{2+} and $UO(OH)^{2+}$ carry charges of +0.001 and −0.057 e, respectively, whereas the hydrogen-bound oxygen centers of $UO(OH)^{2+}$ and $U(OH)_2^{2+}$ draw negative charge from the polar OH bond, resulting in partial charges of −0.41 and −0.47 e, respectively. Consequently, the Coulomb field of the uranium center (∼+2.0 e) is reduced, resulting in a lower polarization of the surrounding solvent and hence a smaller solvation energy of $UO(OH)^{2+}$ and $U(OH)_2^{2+}$ compared to UO_2^{2+}.

Finally, comparison of the three density functionals in Table 4 (LDA, two types of GGA) shows that model M1

(56) Onsager, L. *J. Am. Chem. Soc.* **1936**, *58*, 1486−1493.

Table 4. Solvation Energy[a] (kcal/mol) of Uranyl UO_2^{2+} Calculated with the Three Solvation Models M1−M3 for Various Exchange-Correlation Functionals

	M1	M2[b]	M3[b]
VWN	−296	−321	
BP	−297	−264	−422
PBEN[c]	−298	−253	−407

[a] Models M1−M3 are described in the text. [b] Values calculated for $[UO_2(H_2O)_5]^{2+}$. [c] Reference 14.

yields rather similar values, −297 ± 1 kcal/mol; larger discrepancies were found for the models M2 and M3. Recall that M2 represents the binding energy of a shell of aquo ligands and M3 includes it implicitly. The values calculated with the two GGA functionals, −264 and −253 kcal/mol (M2), differ by 11 kcal/mol, the corresponding M3 values, −422 and −407 kcal/mol, differ by 15 kcal/mol (M3); not unexpectedly, the VWN result, −319 kcal/mol (M2), is larger in absolute size than the GGA values, by ∼50 kcal/mol. In general, one expects the gradient-corrected functionals, BP and PBEN, to yield more reliable energetics;[26,27] however, it is difficult to judge which of the two used here provides better agreement with experiment, because the experimental free energy of hydration of uranyl can only roughly be estimated to lie in the interval[57] of −437 to −318 kcal/mol (see the discussion below).

Several earlier experimental[5,40,58,59] and theoretical[1,3,4,6] studies addressed the preferred number of water ligands of UO_2^{2+}, for which the value of 5 is now generally agreed upon.[1−6,14,40,58,59] Our values of $\Delta G_{298}^{sol,total}$ suggest that penta- and hexacoordinated species should be about equally favored. Inspection of Table 2 shows that complexes with 5 aquo ligands have the most negative binding or solvation energy when higher symmetries (D_{nh} or C_{nv}) are imposed. When lower symmetries (D_{3d} and C_{3v}) are used for the hexacoordinated complexes, their gas-phase binding energies become significantly more negative and total hydration energies $\Delta G_{298}^{sol,total}$ become comparable to those of the corresponding pentacoordinated complexes (Table 2).

The calculated values of $\Delta G_{298}^{sol,total}$ for $[UO_2(H_2O)_6]^{2+}$, $[UO(OH)(H_2O)_6]^{2+}$, and $[U(OH)_2(H_2O)_6]^{2+}$ are −423, −380, and −366 kcal/mol, respectively. As mentioned above, reducing the symmetry of pentaaquo complexes resulted in a less significant energy lowering. The corresponding total free energies of hydration are −422, −388, and −370 kcal/mol. Earlier studies[4,6] at the BLYP and HF levels mainly addressed conformers of $[UO_2(H_2O)_5]^{2+}$ and found only small energetic gains (below 1 kcal/mol) with respect to the D_{5h} structure, in agreement with our work.

No such analysis was previously carried out for $[UO_2(H_2O)_6]^{2+}$. Authors who apparently used the D_{6h} symmetric structure[1,6] concluded that the hexaaquo complex is less favored in the gas phase by 3−4 kcal/mol compared to the pentaaquo complex. Hay et al.,[4] who optimized all complexes without symmetry constraints, found $[UO_2(H_2O)_6]^{2+}$ to be 22 kcal/mol more stable in the gas phase than $[UO_2(H_2O)_5]^{2+} + H_2O$, which concurs with the value of 16 kcal/mol determined in this work. Thus, gas-phase binding energies do not support the generally accepted pentacoordination of uranyl as the preferred complex. Nevertheless, inclusion of electrostatic solvent effects reduces the energy gap between penta- and hexacoordinated complexes. Hay et al. found the pentaaquo complex to be preferred in solution by 1.5 kcal/mol. Our study predicts the two $\Delta G_{298}^{sol,total}$ values to be essentially the same; however, inclusion of thermal and ZPE corrections (see above) is expected to favor the pentaaquo complexes by a few kcal/ mol.[4]

Direct experimental measurements of the free energy of hydration of UO_2^{2+} are not available. Marcus[51] first estimated its hydration enthalpy, $\Delta_h H°(UO_2^{2+})$, at −325.3 ± 5.5 kcal/mol using $\Delta_f H°(UO_2^{2+}(aq,conv)) = -248.8 \pm 1.2$ kcal/mol and $\Delta_f H°(UO_2^{2+}(g)) = 289.2 \pm 4.8$ kcal/mol, calculated from complex thermodynamic cycles.[51] He also estimated the entropy of hydration of uranyl as $\Delta_h S°(UO_2^{2+}) = -78.6$ cal/(mol K) by taking $S°(UO_2^{2++}(aq,conv)) = -23 \pm 0.5$ cal/(mol K) and $S°(UO_2^{2+}(g)) = 62.1 \pm 0.5$ cal/(mol K); these values are consistent with recent thermodynamic data.[52,60] From known hydration enthalpy and entropy values, one obtains the free energy of hydration of uranyl $\Delta_h G°(UO_2^{2+}) = -301.9 \pm 5.5$ kcal/mol. With subsequent measurements, this result can be modified. The latest recommended value for $\Delta_f H°(UO_2^{2+}(aq,conv))$, −243.6 ± 0.6 kcal/mol,[61] changes the value of the free energy of hydration of UO_2^{2+} to $\Delta_h G°(UO_2^{2+}) = -296.6 \pm 5.3$ kcal/mol. A recent experiment[62] restricts the enthalpy of formation of $UO_2^{2+}(g)$ to the interval from 311 to 430 kcal/mol, much above the value estimated by Marcus, 289 ± 5 kcal/mol.[51] With that result, the free energy of hydration of UO_2^{2+} is calculated to lie in the interval $-437 \text{ kcal/mol} < \Delta_h G°(UO_2^{2+}) < -318$ kcal/mol.

Although quantitative agreement with experiment was not expected from the approximate models used here, our best estimate for the free energy of solvation of UO_2^{2+}, −420 kcal/mol, corrected by an estimated value of $\Delta^* \approx +50$ kcal/mol to −370 kcal/mol, falls inside the interval −437 to −318 kcal/mol derived above on the basis of most recent experimental data. Evidently, the rather large uncertainty in the heat of formation of uranyl calls for new measurements or for accurate calculations.

Oxidation and Reduction of Uranium Complexes. Vallet et al.[17] studied the oxidation−reduction properties of uranyl derivatives employing model reactions R1 and R2. Although the naturally preferred forms of U(V) and U(IV) are UO_2^{+} and U^{4+}, these authors chose to consider $UO(OH)^{2+}$ and $U(OH)_2^{2+}$ in their model reaction schemes.

(57) The experimental value cited in ref 14, −402 ± 60 kcal/mol, is in fact the enthalpy of hydration of uranyl.

(58) Åberg, M.; Ferri, D.; Glaser, J.; Grenthe, I. *Inorg. Chem.* **1983**, *22*, 3986−3989.
(59) Thompson, H. A.; Brown, Jr., G. E.; Parks, G. A. *Am. Mineral.* **1997**, *82*, 483−496.
(60) Rizkalla, E. N.; Choppin, G. R. In *Handbook on the Physics and Chemistry of Rare Earths*; Gschneider, K. A., Eyring, L., Choppin, G. R., Lander, G. H., Eds.; Elsevier: Amsterdam, 1994; Vol. 18, pp 529−558.
(61) Cox, J. D.; Drowart, J.; Hepler, L. G.; Medvedev, V. A.; Wagman, D. D. *J. Chem. Thermodyn.* **1978**, *10*, 903−906.
(62) Cornehl, H. H.; Heinemann, C.; Marcalo, J.; de Matos, A. P.; Schwarz, H. *Angew. Chem., Int. Ed. Engl.* **1996**, *35*, 891−894.

Table 5. Reaction Energies $\Delta_R E_0$ and Free Energies $\Delta_R G_{298}$(M1, M3) (kcal/mol) of the First (Eq R1) and Second (Eq R2) Reduction Steps of Uranyl with Water: Comparison of the Results Calculated with Hartree−Fock-Based Correlated Methods and Density Functional Methods for Models with *n* Explicit Aquo Ligands[a]

	eq R1[b]				eq R2[c]			
method	$n = 0$	$n = 4$	$n = 5$	$n = 6$	$n = 0$	$n = 4$	$n = 5$	$n = 6$
ACPF[d]	10.6[f]				5.6[f]			
CASPT2[d]	12.2[f]				4.3[f]			
CCSD(T)[d]	11.9[f]							
B3LYP[d]	−9.4[f]				−0.2[f]			
VWN[e]	−16.0[f]	22.2[h]	24.5[h]	33.5[h]	11.7[f]	25.2[h]	23.7[h]	14.2[h]
BP[e]	−9.5[f]	14.8[h]	19.0[h]	28.5[h]	7.3[f]	19.4[h]	18.8[h]	16.3[h]
BP + CM[e]	9.1[g]		28.2[i]	36.8[i]	36.1[g]		28.9[i]	25.3[i]

[a] Depending on the model, 0−6 aquo ligands were coordinated to uranyl derivatives. [b] Equation R1: $UO_2^{2+} + 1/2H_2O = UO(OH)^{2+} + 1/4O_2$. [c] Equation R2: $UO(OH)^{2+} + 1/2H_2O = U(OH)_2^{2+} + 1/4O_2$. [d] Reference 17. [e] This work. [f] $\Delta_R E_0$. [g] $\Delta_R G_{298}$(M1). [h] $\Delta_R G_{298}$(M2). [i] $\Delta_R G_{298}$(M3).

This choice has the advantage of minimizing the differential effects between gas-phase and solvated models. In the following, we will show that even for reactions so carefully balanced, solvation effects can be quite important.

We employed LDA (VWN) and GGA (BP) density functionals, in combination with various solvation models, mainly to estimate the change of reaction energies due to solvation. The reaction energies $\Delta_R E_0$ for (R1) and (R2) were calculated first in the gas phase and then corrected (in single-point fashion) for solvation effects according to the three models described above: pure CM (M1); explicit water ligands (M2); a combination approach (M3). The following set of equations shows the relationship of these quantities to the solvation energies discussed above:

$$\Delta_R G_{298}(\mathrm{M1}) = \Delta_R E_0 + \sum_{\text{products}} \Delta G_{298}^{\mathrm{CM}} - \sum_{\text{reactants}} \Delta G_{298}^{\mathrm{CM}} \quad (4)$$

$$\Delta_R G_{298}(\mathrm{M2}) = \Delta_R E_0 + \sum_{\text{products}} \Delta E_{\mathrm{binding},0}^{(\mathrm{g})} - \sum_{\text{reactants}} \Delta E_{\mathrm{binding},0}^{(\mathrm{g})} \quad (5)$$

$$\Delta_R G_{298}(\mathrm{M3}) = \Delta_R E_0 + \sum_{\text{products}} \Delta G_{298}^{\mathrm{sol,total}} - \sum_{\text{reactants}} \Delta G_{298}^{\mathrm{sol,total}} \quad (6)$$

In Table 5, we compare reaction energies at 0 K calculated previously[17] to the corresponding results of this work. Reaction energies obtained previously with different quantum chemistry methods (Hartree−Fock-based correlated methods and density functional methods) scatter from −9.4 to 13.7 kcal/mol for the first reduction step and from −0.2 to 5.7 kcal/mol for the second step.[17]

Of course, it is not rigorously correct to compare energies at 0 K with Gibbs free energies at 298 K. However, for the gas-phase reactions R1 and R2, the differential corrections due to ΔZPE, rotational, vibrational, and translation energy as well as ΔnRT were estimated not to exceed 2−3 kcal/mol.

From Table 5, one can see that the gas-phase BP model predicts the first reduction step to be exothermic by −9.5 kcal/mol in agreement with previous B3LYP results.[17] The second reduction step is calculated 7.3 kcal/mol endothermic, at variance with the former study which obtained −0.2 kcal/mol. The solubility of U(IV) species is smaller than that of U(VI) complexes, and therefore, the free energies of reduction in solution are larger (more positive) than those of the corresponding reactions in the gas phase.

With a pure CM treatment (no explicit aquo ligands), the free energy of the first step increases by 18.6 kcal/mol, from −9.5 to 9.1 kcal/mol, and that of the second step by 18.8 kcal/mol, from 7.3 to 36.1 kcal/mol. The combined solvation model M3 furnishes an endoergicity of 28−37 kcal/mol for the first and 25−29 kcal/mol for the second step. Comparison of these results shows that the pure CM (M1) underestimates the reaction endoergicity of (R1) by 10−20 kcal/mol and overestimates reaction endoergicity of (R2) by about 10 kcal/mol. These discrepancies occur despite the fact that our model reactions are quite balanced: they feature the same number of aquo ligands, and one would expect that the effects of their covalent bonding would largely cancel. The purely quantum-chemical model M2 for ions with 5 or 6 aquo ligands underestimates the reaction free energies by about 10 kcal/mol.

When solvation effects are treated with the combination model M3, the reaction free energies of the first (eq R1) and second (eq R2) reduction step change by 38−47 and 18−22 kcal/mol, respectively, compared to the gas-phase results ($n = 0$). In other words, the environmental effect is comparable in size or even larger than the difference of density functional and correlated HF results.[17] Clearly, solvation effects are crucial for predicting enthalpies of experimentally relevant reactions of uranyl and other actinide complexes.

Conclusions

Solvation of UO_2^{2+}, $UO(OH)^{2+}$, and $U(OH)_2^{2+}$ was studied systematically using three levels of approximation: direct treatment with a continuum model (M1); explicit quantum-chemical treatment of the first hydration sphere, i.e., the complexes $[UO_2(H_2O)_n]^{2+}$, $[UO(OH)(H_2O)_n]^{2+}$, and $[U(OH)_2(H_2O)_n]^{2+}$ ($n = 4-6$) without further reference to the solvent (M2); their combination (M3). Models M1 and M2 were found to recover the solvation energy only partially, underestimating it by 75−100 and 140−160 kcal/mol, respectively. At variance with previous theoretical studies that assumed "high-symmetry" complexes[1,3,6] but in agreement with Hay et al.,[4] the hexacoordinated uranyl was found energetically favored over $n = 4$ and 5 with model M2, whereas the five-ligand complex becomes about equally preferred with a

solvation treatment of type M3. Inclusion of thermal and ZPE corrections would imply a relative stabilization of the pentaaquo complex by up to 10 kcal/mol. The structure of the complex $[UO_2(H_2O)_5]^{2+}$ optimized with the VWN density functional was determined in good agreement with results of EXAFS experiments.[5]

The hypothetical reduction of U(VI) by water (reactions R1 and R2) was studied by density functional methods and various solvation treatments. This redox model was previously investigated[17] in the gas phase at various correlated levels of theory. Net reaction enthalpies computed by different methods scattered by ~25 kcal/mol. Here, we demonstrated that the correction due to solvation may amount to as much as ~60 kcal/mol for the full reduction U(VI) → U(IV). This correction is significantly larger than the discrepancies among the various gas-phase results and should not be ignored when comparing with experiments, even at a qualitative level. Solvation is actually the main reason for the strong endoergicity of both reduction steps. Spin−orbit effects, neglected in our calculations, were estimated to reduce the net endoergicity by ~13 kcal/mol.[17]

Finally, we add a few remarks about the implications of the current results for the stability of various oxidation states of U under natural conditions. Our models successfully predict the stability of U(VI) with respect to reduction by water. They also imply that U(VI) is the preferred form in aqueous solution due to its better solubility compared to U(V) and U(IV) species. However, the endoergicity of reactions R1 and R2 does not imply that U(V) and U(IV) species are unstable in water solution. To clarify this point, one needs to consider the reactions

$$\mathrm{U(VI)} \xrightarrow{+\,H_2O} \mathrm{U(V)} \xrightarrow{+\,H_2O} \mathrm{U(IV)}$$

The experimental standard redox potentials[63] of the couples UO_2^{+}/U^{4+} and UO_2^{2+}/UO_2^{+}, 0.38 and 0.17 eV, clearly entail that U^{4+} and UO_2^{+} are stable with respect to oxidation by H_2O (recall that the standard redox potential for the couple $H^{+}/1/2H_2$ is 0 eV and the pH dependence of this potential is negative). In natural aqueous environments in contact with the atmosphere, U(IV) will, of course, undergo a slow oxidation by molecular oxygen and other oxidants.

Acknowledgment. We thank F. Schlosser for assistance with some calculations. We acknowledge stimulating discussions with him as well as with A. V. Matveev, A. A. Voityuk, and V. Vallet. L.V.M. is grateful for a fellowship of the Alexander von Humboldt Foundation. This work was supported by the Bundesministerium für Wirtschaft und Arbeit (Grant No. 02E9450) and Fonds der Chemischen Industrie.

Supporting Information Available: Listings of total energies, hydration energies, and Cartesian coordinates of various conformers of $[UO_2(H_2O)_n]^{2+}$, $[UO(OH)(H_2O)_n]^{2+}$, and $[U(OH)_2(H_2O)_n]^{2+}$. This material is available free of charge via Internet at http://pubs.acs.org.

IC035450H

(63) Silva, R. J.; Nitsche, H. *Radiochim. Acta* **1995**, *70*, 377−396.